Development of Artificial Intelligence-based Real-time Automatic Fusion of Multiparametric Magnetic Resonance Imaging and Transrectal Ultrasonography of the Prostate

Francesco Cianflone, Bogdan Maris, Riccardo Bertolo, Alessandro Veccia, Francesco Artoni, Greta Pettenuzzo, Francesca Montanaro, Antonio Benito Porcaro, Alberto Bianchi, Sarah Malandra, Francesco Ditonno, Maria Angela Cerruto, Giulia Zamboni, Paolo Fiorini, and Alessandro Antonelli

OBJECTIVE To report the development of artificial intelligence (AI)-based software to allow for the autonomous fusion of transrectal ultrasound and multiparametric magnetic resonance images of the prostate to be used during transperineal prostate biopsies.

MATERIALS AND METHODS This study was approved by the Institutional Review Board (protocol ID 3167CESC). The automatic software development for fusion biopsy involved 3 steps: (1) developing an AI component to segment the prostate during ultrasound; (2) developing the component to segment anatomical structures in magnetic resonance images using labeled datasets from the Cancer Imaging Archive and in-house scans; (3) developing the fusion component to register segmented ultrasound and magnetic resonance images using a 3-step process: pre-alignment, rigid alignment, and elastic fusion, validated by measuring the lesion distance between modalities. Statistical analysis included descriptive statistics and the Mann-Whitney *U* test, evaluating outcomes with Dice scores and average precision metrics.

RESULTS The ultrasound component showed a Dice score of 0.87 with a test set of 75,357 images and 28,946 annotations. The magnetic resonance component achieved a Dice score of 0.85 on a test set of 2494 images and annotations. It also demonstrated a mean average precision of 0.80 for bounding boxes and 0.88 for segmented objects, both measured at a 50% intersection over union threshold. The fusion AI component reduced the median magnetic resonance-ultrasound lesion distance from 8 mm (interquartile ranges 6-9) after rigid fusion to 4 mm (interquartile ranges 3-5) after elastic fusion (P <.001).

CONCLUSION A data processing pipeline and AI were created to allow for the autonomous fusion of ultrasound and magnetic resonance images to be ideally used during transperineal prostate biopsies. UROLOGY 199: 27–34, 2025.

Biopsy remains an essential step in the diagnosis of prostate cancer (PCa). For a decade, the routine implementation of multiparametric magnetic resonance imaging (mpMRI) in PCa diagnosis has revolutionized the framework of prostate biopsy,[1,2] allowing systematic templated sampling to be paired with targeted sampling of suspicious areas detected on mpMRI.[3,4]

Such targeted sampling implies identifying the areas of suspect revealed by mpMRI on the real-time image provided by transrectal ultrasound (TRUS) during prostate biopsy. The method can be cognitive or software-based: the first relies solely on the operator's awareness of the most suspicious area's location, while the latter provides a true overlay (also called "*fusion*") of the suspicious mpMRI image with the real-time image

Francesco Cianflone and Bogdan Maris contributed equally.

From the Department of Surgery, Dentistry, Pediatrics and Gynecology, Urology Unit, Azienda Ospedaliera Universitaria Integrata, University of Verona, Verona, Italy; the Department of Engineering for Innovation Medicine, University of Verona, Verona, Italy; and the Department of Diagnostic and Public Health, Unit of Radiology, Azienda Ospedaliera Universitaria Integrata, University of Verona, Verona, Italy

Address correspondence to: Riccardo Bertolo, MD, PhD, Azienda Ospedaliera Universitaria Integrata Verona, AUOI Verona, Borgo Trento Hospital, University of Verona, Piazzale A. Stefani 1, 37126 Verona, Italy.

E-mail: riccardogiuseppe.bertolo@univr.it

Submitted: September 23, 2024, accepted (with revisions): March 4, 2025

obtained during the TRUS performed while taking the biopsy.

To date, evidence shows no superiority between software-based and cognitive fusion.[5-7] Possible explanations include the operators' expertise, the patient's movements during the procedure, the target visibility, and the quality of the software used to "fuse" the target mpMRI lesion with the real-time TRUS performed during the biopsy.[8]

Recent experiences have pioneered using artificial intelligence (AI) in this context.[9,10] Although potentially more precise in identifying target areas, these methods equally suffer from potential bias during the overlapping to real-time TRUS images. To contribute to this field, our research group conceived an algorithm to achieve real-time prostate segmentation on TRUS, which could allow prostate tracking during the procedure, with the goal of compensating both the ultrasound probe and the patient's movements. The real-time AI-driven matching between segmented TRUS images and segmented mpMRI images would provide a sound framework for autonomous fusion during transperineal biopsy that could overcome most of the limitations experienced during this procedure. Herein, we present the development of a data processing pipeline and AI to allow for the autonomous fusion of TRUS and mpMRI images to be ideally used during transperineal prostate biopsies.

MATERIALS AND METHODS

The study protocol obtained Institutional Review Board approval (protocol ID 3167CESC).

The 3 steps for the development of the automatic software to be used during fusion biopsy consisted of

1. Developing the TRUS AI component to process data streams from the ultrasound machine to perform the segmentation of the prostate during the initial exploration.
2. Developing the mpMRI AI component to process the specific patient images loaded from the digital imaging and communications in medicine (DICOM) or the picture archiving and communication system components to segment the relevant anatomical structures.
3. Developing the fusion AI component to perform the registration between the segmented TRUS images and the mpMRI segmented images, both fused into their respective volumes.

Development of Each of the Components: Methodology

TRUS AI Component. For this study, prostate sagittal and axial ultrasound images (frame rate ~20Hz) were recorded in DICOM format using an Arietta V70 ultrasound machine (Hitachi, Tokyo, Japan) with a biplanar transrectal probe. Hundreds of images were collected for each prostate TRUS from a cohort of patients who underwent prostate TRUS between April 2021 and July 2022 as part of the diagnostic pathway for PCa (COHORT 1).

The prostates were contoured on each sagittal and axial scan recorded from COHORT 1, using a semi-automatic interface in Mevislab (MeVis Medical Solutions AG, Bremen, Germany). This process allowed to obtain the so-called "ground truth," a set of images with verified and labeled prostate contours. Segmentation was performed by 3 radiologists under the supervision of an expert radiologist with over 20 years of experience in both clinical practice and research.

At this point, *PROST-Net*, a deep-learning model designed for real-time prostate contouring, was run. The model works by (1) detecting the prostate, (2) isolating a region of interest, and (3) contouring that region.[11] We applied PROST-Net to the set of labeled ultrasound images from COHORT 1. As per standard practice in AI development, this set was divided into training, test, and validation subsets with a ratio of 60%, 20%, and 20%, respectively.[12] After this step, we renamed PROST-Net as "*PROST-Net TRUS-trained*" on TRUS.

In the next step, "PROST-Net TRUS-trained" was run on a second set of prostate sagittal and axial ultrasound images recorded in DICOM format using a different ultrasound machine (Esaote, Genoa, Italy) collected from a cohort of patients who underwent prostate TRUS between February 2023 and June 2023 as—again—part of the diagnostic pathway for PCa (COHORT 2). The adoption of a different ultrasound machine to obtain the images from COHORT 2 was aimed at improving the robustness of the learning model across varied types of equipment used.

The segmentations performed by "PROST-Net TRUS-trained" autonomously on the set of images from COHORT 2 were manually adjusted by the same radiology team to fine-tune the "PROST-Net trained" output. "PROST-Net TRUS-trained" was then applied to the set of segmentations on ultrasound images from COHORT 2 manually adjusted by the urologists. The Dice similarity coefficient measured the overlap between the manually relabeled prostate and the prostate identified by the "PROST-Net trained." After this step, we renamed "PROST-Net TRUS-trained" as "PROST-Net TRUS-trained2."

The development pipeline from PROST-Net to PROST-Net TRUS-trained2 for TRUS is summarized in Figure 1A.

mpMRI AI Component. To train PROST-Net to contour the prostate on mpMRI images, we used a set of T2-weighted mpMRI scans archived on the Cancer Imaging Archive website (https://www.cancerimagingarchive.net).[13] On this resource, expert annotations and segmentations of prostate mpMRIs were already available and used as "ground truth." Thus, the step of contouring by human hands was not needed. We applied *PROST-Net* to the set of labeled mpMRI images from the

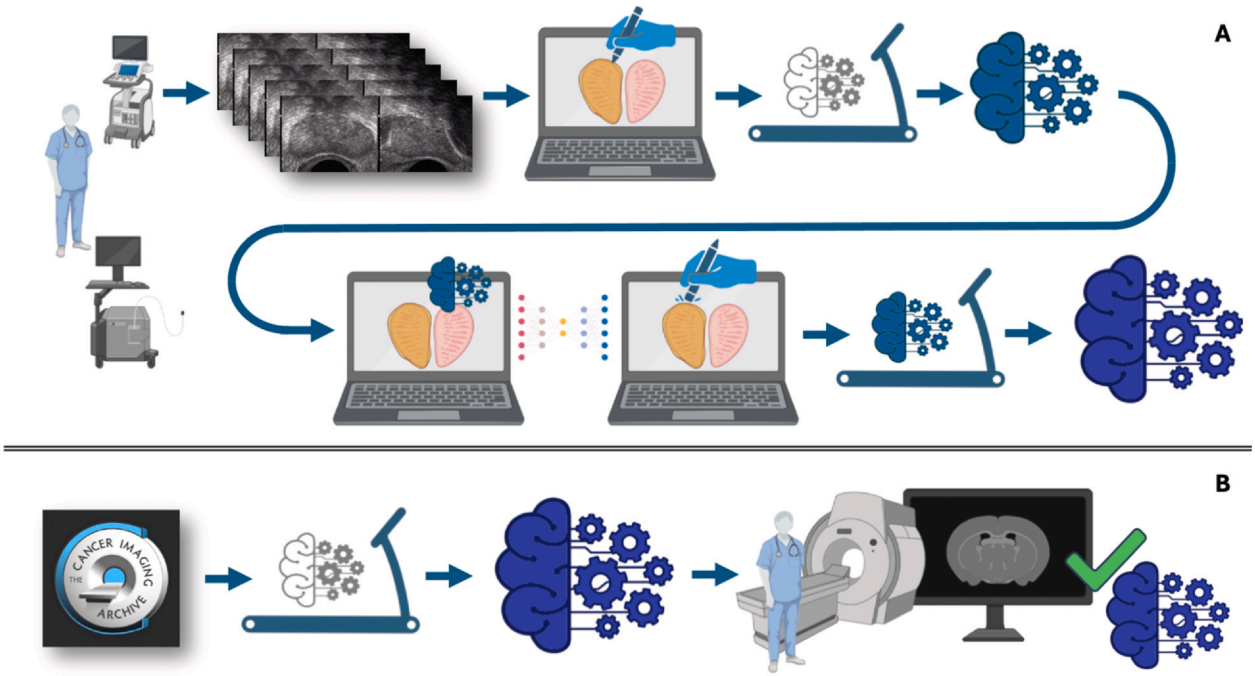

Figure 1. **(A)** Development of the TRUS AI component: prostate TRUS images obtained from institutional patients (COHORT 1) were contoured manually to create a "ground truth" → PROST-Net was trained and validated on these images (PROST-Net trained) and then applied to another set of images from obtained from a different ultrasound machine → the model's output was fine-tuned → PROST-Net trained was then retrained (PROST-Net trained^{trained}). **(B)** Development of the mpMRI AI component: PROST-Net was trained on labeled T2-weighted mpMRI scans obtained from the Cancer Imaging Archive (PROST-Net trained) → PROST-Net trained was validated on in-house mpMRI scans obtained from COHORT 1 patients.

Cancer Imaging Archive website. After this step, PROST-Net became "*PROST-Net MRI-trained*" on mpMRI.

The accuracy of "PROST-Net MRI-trained" was validated by using previously contoured in-house mpMRI scans performed on COHORT 1 patients. The Dice similarity coefficient measured the overlap between the manually labeled prostate and the prostate identified by the PROST-Net MRI-trained. The development pipeline from PROST-Net to *PROST-Net MRI-trained* for mpMRI is summarized in Figure 1B.

Fusion AI Component. Finally, a fusion algorithm was designed and integrated into the respective trained versions of PROST-Net after dedicated training on the identification and segmentation of the prostate on TRUS and mpMRI images. For this step, pairs of TRUS images and corresponding mpMRI of prostates with suspicious lesions (PIRADS 3 or higher) available on the Cancer Imaging Archive website were used.[13] In these images, both the prostate and the lesion were already segmented in both the TRUS and the corresponding mpMRI. Specifically for this step, all the data were exported from DICOM in ".nrrd" (near raster raw data) three-dimensional (3D) format.

The fusion process worked in 3 steps: pre-alignment, rigid alignment, and elastic fusion.

Given as input the TRUS and mpMRI images, both as 3D volumes represented as grids of voxels in grayscale, along with their respective segmentations of the prostate gland, the algorithm transformed the mpMRI dataset (both image and segmentation) so that it corresponded to the TRUS volume.

Pre-alignment. In this phase, the algorithm performed an initial alignment based on bringing the images to the same dimension and resolution. The algorithm also updated the spatial information into a 3D visualization tool to align the 3D segmentations of the pairs of prostates at TRUS and mpMRI to have the same "*centroid*." When aligning 2 or more objects or images, the centroid can be used as a reference point or a measure of position (Supplementary Fig. 1A, B).

Rigid Fusion. In this phase, the algorithm outputs a rotation and a translation, which were applied to the mpMRI image. The rigid transform was obtained through an optimization process. The algorithm's input was a fixed image (TRUS) and an in-motion image (mpMRI), as well as parameters such as optimization metric, type of optimization, and interpolation. The optimization process updated the transform so that the in-motion image was aligned with the fixed image using the predefined distance metric (Supplementary Fig. 1C, D).

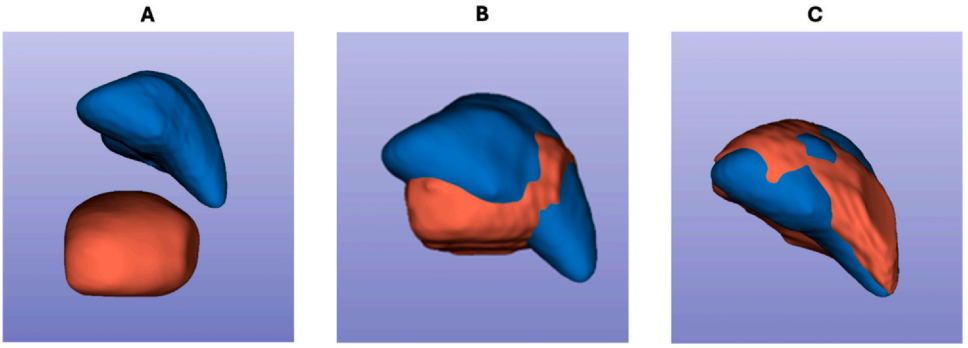

Figure 2. 3D models of a segmented prostate **(A)** before fusion; **(B)** after pre-alignment; **(C)** after elastic fusion (mpMRI: red, TRUS: blue).

Elastic Fusion. The input of this phase was the prostate segmentations. From these segmentations, the algorithm generated a distance map image. The distance map created from the TRUS image was kept fixed, while the mpMRI distance map was moving. The output transform was applied to the mpMRI image and its associated segmentation. The results were optimized by a B-spline function, which smoothly aligned the 2 segmentations so that their area in the image overlapped. In contrast, the external area of the prostate in the transformed mpMRI image was very deformed (Supplementary Fig. 2, Fig. 2).

The quality of the fusion of the images was assessed by measuring the distance (in mm) between the lesion on mpMRI and the corresponding lesion on TRUS.

Statistical Analysis

Descriptive statistics were used to characterize the study cohort: medians and interquartile ranges (IQR) were used to report continuous data. The Mann-Whitney *U* test was used to test the differences between distributions of continuous variables. The outcomes measured were

1. The Dice score is a metric for evaluating image segmentation algorithms. It measures the overlap between predicted and ground truth segmentations, with a higher score indicating better accuracy.[14]
2. The Dice score per patient, calculated on 3D volumes instead of two-dimensional images, reporting also its standard deviation.
3. bbox_mAP_50 and segm_mAP_50, commonly used evaluation metrics in object detection and instance segmentation tasks, respectively.[15] They measure the mean average precision (mAP) at a 50% intersection over union threshold for bounding boxes (bbox_mAP_50) and segmented objects (segm_mAP_50). These metrics provide insights into the accuracy of object localization and segmentation, with higher values indicating better performance. More specifically, the mAP at a 50% intersection over union threshold indicates how well the system can detect and locate objects with at least a 50% overlap accuracy.

RESULTS

Transrectal Ultrasound AI

Data from 292 subjects were employed to train the TRUS AI component. The median age at TRUS was 67 (IQR 64-71). The median prostate volume at TRUS was 48.6 mL (IQR 35.7-62.3). The test split contained 75,357 images and 28,946 annotations. The train split contained 548,041 images and 210,126 annotations. The validation split contained 61,654 images and 23,541 annotations. The Dice score, the Dice score per patient, the bbox_mAP_50, and the segm_mAP_50 were 0.87 (IQR were 0.83-0.9, 0.83-0.91, 0.84-0.9, and 0.83-0.9, respectively). Moreover, the median computation time for TRUS slices segmentation of a whole prostate is 0.05 second (IQR 0.04-0.06).

Multiparametric Magnetic Resonance Imaging AI

MRI data from all 1151 subjects in the Cancer Imaging Archive dataset[13] were employed in developing this component. Test split contained 2494 images and 2494 annotations. The train split contained 47,376 images and 47,376 annotations. The validation split contained 496 images and 496 annotations. The Dice score and the Dice score per patient were 0.85 (IQR were 0.85-0.92 and 0.84-0.92, respectively). The bbox_mAP_50 was 0.89 (IQR 0.84-0.9). The segm_mAP_50 was 0.88 (IQR 0.82-0.91). Notably, the median computation time for whole MRI 3D segmentation was 1 second (IQR 0.98-1.01).

Fusion AI

To develop the fusion AI component, MRI, TRUS, and lesions data from all 1151 subjects available in the Cancer Imaging Archive dataset[13] were employed. The median mpMRI-ultrasound lesion distance was 8 mm (IQR 6-9) after the rigid fusion and 4 mm (IQR 3-5) after elastic fusion ($P < .001$). The variability was attributed to cases where the tumor segmentation on mpMRI

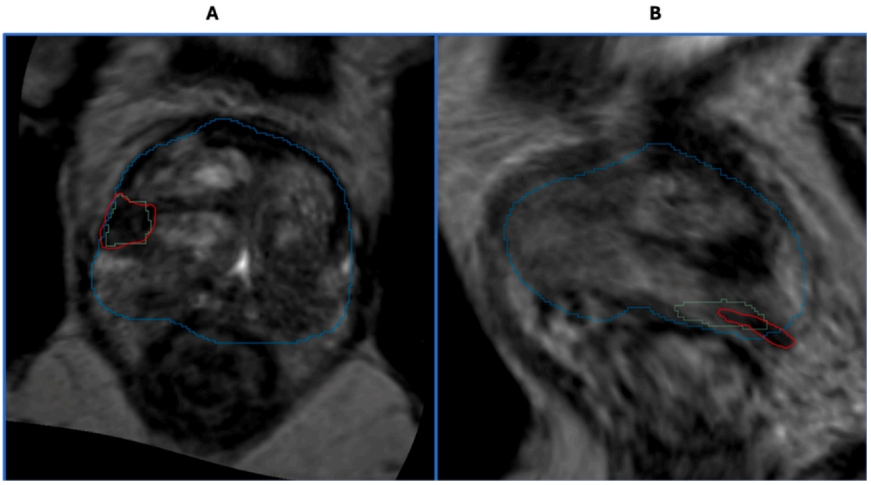

Figure 3. **(A)** mpMRI after elastic fusion with the tumor (green on mpMRI, red on the corresponding lesion on TRUS) and the prostate (blue) contoured. The darker area of the tumor coincides with the tumor at TRUS; **(B)** example of partial overlapping of the tumor at TRUS with the tumor at mpMRI, after elastic fusion.

coincided with that on TRUS (Fig. 3A) and cases where the overlap was only partial (Fig. 3B). Moreover, out of a total of 1617 lesions, 1036 (64%) had a diameter greater than 5 mm; in this subset of patients, the median diameter was 15.6 mm (IQR 11.4-19.1 mm). Remarkably, the median computation time for the fusion algorithm was 4 seconds (IQR 3.97-4.02).

DISCUSSION

In the present study, we reported the development of a data processing pipeline and subsequent AI training to allow for the real-time autonomous fusion of TRUS and prostate mpMRI images to be ideally used during transperineal prostate biopsies.

Today, AI is under investigation at many steps in the diagnostic pathway of PCa.[16,17] Some authors reported developing an AI to help in prostate segmentation, either whole gland or segmental, in different settings ranging from prostate mpMRI to MRI- and computed tomography-guided prostate radiotherapy.[18-23] However, only 2 reports, one published in 2021 and one in 2024, focused on the accuracy of AI segmentation compared to a manual one. While their results were conflicting, the latter report was more favorable toward AI, and, in the authors' opinion, the rapid pace of development in this field should not be overlooked when assessing the existing literature.[24,25]

Other authors have reported the development of AI models to address different shortcomings in the diagnostic pathway of PCa. Some strived to automatize the recognition of significant cancerous lesions on mpMRI scans[9] or on ^{68}Gallium-prostate-specific membrane antigen positron emission tomography images.[26] In the first case, the authors developed a closed-loop AI that outperformed or matched the performance of more than 70% of general readers in the MRI assessment of PCa.[9] A convoluted neural network (CNN) was developed in the latter that automatically segmented intraprostatic cancer lesions with a median dice score of 0.74.[26] Moreover, another group tried developing an AI to assess PCa's extraprostatic extensions,[10] while others aimed to aid PCa classification[27] or to correlate mpMRI features to histopathology.[28] In the first case, the model demonstrated a sensitivity of 0.67, specificity of 0.73, and accuracy of 0.72 compared to the radiologist's sensitivity of 0.81, specificity of 0.62, and accuracy of 0.66; using histopathology as the ground truth, the model exhibited slightly lower sensitivity but outperformed the radiologist in specificity and overall accuracy.[9] In the second case, a CNN was developed and showed no significant differences and was equivalent to the radiologists in classifying suspicious lesions, which could enhance the diagnostic capabilities of an inexperienced radiologist.[27] In the last case, a CNN was developed that could predict histology data without any significant difference compared to manual segmentations from MRI.[28]

Most AI models developed for prostate segmentation are CNN-based on the U-Net architecture.[18-23] Our model, PROST-Net,[11] comprises a backbone part, which uses ResNet101 or ResNet50, the Region Proposal Network for selecting the region of interest, and the head of the network, which outputs the segmentation mask and is U-Net inspired.[29-32] This gives our AI good flexibility to be applied to different input sources.

The sole effort reported on AI utilization in ultrasound scans of the prostate, particularly during TRUS, was the study by Andersén et al. In this study, the authors employed CNNs to evaluate the positions of brachytherapy needles and digitize them. Still, they did not undertake the task of AI-based prostate segmentation on ultrasound images.[33]

Therefore, to our knowledge, ours is the first to report on AI-driven prostate segmentation using ultrasound imaging. As noted before, previous efforts have focused primarily on mpMRI segmentation, leaving a significant gap in real-time ultrasound applications. Furthermore, ours is the first

instance of employing AI in the direction of an autonomous system to achieve real-time fusion of TRUS and mpMRI images, to be ideally used during prostate biopsy.

On purpose, our AI algorithm, PROST-Net, was developed based on prostate images obtained using different ultrasound machines. We believe this underscored its robustness across varied types of equipment used. The reader could argue about the arbitrary splitting of the images used for testing, training, and validation. Machine learning models typically require a substantial amount of data for training to learn the underlying patterns effectively. A split of 20% for testing, 60% for training, and 20% for validation is often used to balance the need for enough training data while ensuring that the model's performance is assessed on separate, unseen datasets to avoid overfitting and to validate its generalizability.[12]

Notably, for developing the TRUS and the mpMRI AI components, the Dice coefficients for prostate segmentation reached a ≥0.85 value, indicating a high degree of overlap.

These significant results demonstrate the potential for high precision when adopted in clinical settings. However, further refinement of the accuracy is necessary before clinical applicability. Moreover, in future development steps, the AI model could be improved by integrating the segmentation and fusion model with mpMRI features,[34,35] and hypothetically with TRUS features as well, to better inform the location and degree of rigid or elastic fusion.

Our approach addresses the limitations identified in previous studies regarding the fusion of mpMRI and TRUS images for prostate biopsies.[8] Unlike cognitive fusion, which relies heavily on operator expertise or existing software-based methods that have not shown superior results, our AI-driven method may offer a more consistent and reliable tool for achieving fusion once refined and validated in a clinical setting. To note, in our experience, the median lesion distance was significantly reduced from 8-4 mm following elastic fusion ($P < .001$). However, as much as this is a good result in favor of elastic over rigid fusion, a misalignment of just a few millimeters can still be an issue in this setting and a potential cause of missing the target (ie, cancer).

Previous studies have demonstrated the accuracy of fusion biopsy to be approximately 3 mm.[36] In addition, when assessing cognitive vs software-based fusion targeted biopsy, many studies could not find any superiority of the latter technique, with the detection rate of clinically significant PCa on targeted biopsies ranging from 59%-78%.[37-39] However, some studies have suggested a superiority of software-based fusion, as would be expected.[40,41] Certainly, the operator's learning curve is important and may have an impact in this regard.[42]

While we lack data on the relationship between accuracy and lesion diameter, considering a median error of the fusion algorithm of 4 mm and the lesions with a >5 mm diameter (which constitute 64% of the total lesions), we can infer that almost all these larger lesions might be reached. However, we acknowledge that the system might fail when targeting smaller lesions.

A strength of our study is the inclusion of 2 sets of TRUS images obtained using different ultrasound machines. We feel this would suggest the algorithm's versatility. Additionally, training our AI on a large, diverse dataset and validating it on in-house mpMRI data adds to the robustness of our findings. In addition, whole prostate TRUS slice segmentation can be performed in real-time, with an average computation time of 0.05 second, comparable to the frame rate acquisition of a ultrasound machine (approximately 20 Hz), while the segmentation of an entire 3D MRI takes around 1 second. Notably, the average computation time for the fusion algorithm was 4 seconds. In our opinion, these computation times are suitable for the clinical setting.

Our study has limitations. Specifically, while the TRUS AI was developed and retrospectively tested on new TRUS data, the MRI and fusion components were trained and tested using the Cancer Imaging Archive dataset.[36] Future studies should focus on validating the complete AI system with TRUS and MRI data from clinical settings. Moreover, while promising, the precision of the current version of the developed AI model is not yet sufficient for immediate clinical implementation. In our opinion, achieving a fusion accuracy expressed by a lesion distance of ≤2 mm should remain the goal for future iterations of our algorithm. Efforts in the future should focus on enhancing the AI model to achieve the desired precision levels. Increasing the dataset size and diversity, as well as continuous validation with clinical data, will be crucial before implementing it in a clinical setting.

CONCLUSION

We developed an effective data processing pipeline and AI to allow for the autonomous fusion of TRUS and mpMRI images to be ideally used during transperineal prostate biopsies. The further goal will be to add data for the AI algorithm to enhance its precision, thus providing a sound basis for developing clinically applicable autonomous fusion software.

Ethical Declarations

Approval of the research protocol by Institutional Reviewer Board ID 3167CESC (Comitato etico Territoriale Area Sud-Ovest Veneto - CET-ASOV, Azienda Ospedaliera Universitaria Integrata Verona c/o UOC Farmacia, P.le Stefani, 1 37126 Verona).

Funding: None.

CRediT Authorship Contribution Statement

Riccardo Bertolo: Writing – review & editing, Validation, Supervision, Methodology. **Alessandro Veccia:** Writing – review & editing, Visualization,

Validation. **Francesco Artoni:** Visualization, Validation, Data curation. **Greta Pettenuzzo:** Visualization, Validation, Data curation. **Francesco Cianflone:** Writing – original draft, Project administration, Methodology, Investigation, Data curation, Conceptualization. **Bogdan Maris:** Validation, Software, Resources, Project administration, Methodology, Investigation, Formal analysis, Data curation, Conceptualization. **Alessandro Antonelli:** Writing – review & editing, Visualization, Validation, Supervision, Project administration, Methodology, Investigation, Conceptualization. **Francesco Ditonno:** Visualization, Validation, Data curation. **Maria Angela Cerruto:** Visualization, Validation, Supervision. **Giulia Zamboni:** Visualization, Validation, Resources, Data curation. **Paolo Fiorini:** Validation, Software, Resources, Project administration, Methodology, Investigation, Conceptualization. **Francesca Montanaro:** Visualization, Validation, Data curation. **Antonio Benito Porcaro:** Visualization, Validation. **Alberto Bianchi:** Visualization, Validation. **Sarah Malandra:** Visualization, Validation, Resources.

Declaration of Competing Interest

The authors declare that they have no known competing financial interests or personal relationships that could have appeared to influence the work reported in this paper.

Acknowledgment

None.

Approval of the Research Protocol by an Institutional Review Board

ID 3167CESC.

Informed Consent

Obtained from all patients.

Registry and the Registration No. of the Study/Trial

N/A.

Animal Studies

N/A.

Appendix A. Supporting information

Supplementary data associated with this article can be found in the online version at doi:10.1016/j.urology.2025.03.004.

References

1. Cornford P, van den Bergh RCN, Briers E, et al. EAU-EANM-ESTRO-ESUR-ISUP-SIOG guidelines on prostate cancer-2024 update. Part I: screening, diagnosis, and local treatment with curative intent. *Eur Urol*. 2024;86:148–163. https://doi.org/10.1016/j.eururo.2024.03.027
2. Bertolo R, Vittori M, Cipriani C, et al. Diagnostic pathway of the biopsy-naïve patient suspected for prostate cancer: Real-life scenario when multiparametric magnetic resonance imaging is not centralized. *Prog Urol*. 2021;31:739–746. https://doi.org/10.1016/j.purol.2020.12.008
3. Porpiglia F, Checcucci E, DE Cillis S, et al. A prospective randomized controlled trial comparing target prostate biopsy alone approach vs. target plus standard in naïve patients with positive mpMRI. *Minerva Urol Nephrol*. 2023;75:31–41. https://doi.org/10.23736/S2724-6051.22.05189-8
4. Rouvière O, Puech P, Renard-Penna R, et al. Use of prostate systematic and targeted biopsy on the basis of multiparametric MRI in biopsy-naive patients (MRI-FIRST): a prospective, multicentre, paired diagnostic study. *Lancet Oncol*. 2019;20:100–109. https://doi.org/10.1016/S1470-2045(18)30569-2
5. Wegelin O, Exterkate L, van der Leest M, et al. The FUTURE Trial: a multicenter randomised controlled trial on target biopsy techniques based on magnetic resonance imaging in the diagnosis of prostate cancer in patients with prior negative biopsies. *Eur Urol*. 2019;75:582–590. https://doi.org/10.1016/j.eururo.2018.11.040
6. Watts KL, Frechette L, Muller B, et al. Systematic review and meta-analysis comparing cognitive vs. image-guided fusion prostate biopsy for the detection of prostate cancer. *Urol Oncol*. 2020;38:734.e19–734.e25. https://doi.org/10.1016/j.urolonc.2020.03.020
7. Wegelin O, van Melick HHE, Hooft L, et al. Comparing three different techniques for magnetic resonance imaging-targeted prostate biopsies: a systematic review of in-bore versus magnetic resonance imaging-transrectal ultrasound fusion versus cognitive registration. is there a preferred technique? *Eur Urol*. 2017;71:517–531. https://doi.org/10.1016/j.eururo.2016.07.041
8. Marra G, Ploussard G, Futterer J, et al. Controversies in MR targeted biopsy: alone or combined, cognitive versus software-based fusion, transrectal versus transperineal approach? *World J Urol*. 2019;37:277–287. https://doi.org/10.1007/s00345-018-02622-5
9. Yu R, Jiang KW, Bao J, et al. PI-RADS^{AI}: introducing a new human-in-the-loop AI model for prostate cancer diagnosis based on MRI. *Br J Cancer*. 2023;128:1019–1029. https://doi.org/10.1038/s41416-022-02137-2
10. Simon BD, Merriman KM, Harmon SA, et al. Automated detection and grading of extraprostatic extension of prostate cancer at MRI via cascaded deep learning and random forest classification. *Acad Radiol*. 2024;31:4096–4106. https://doi.org/10.1016/j.acra.2024.04.011
11. Palladino L, Maris B, Antonelli A, et al. PROST-Net: a deep learning approach to support real-time fusion in prostate biopsy. *IEEE Trans Med Robot Bionics*. 2022;4:323–326.
12. Goodfellow I, Bengio Y, Courville A. *Deep Learning*. MIT Press; 2016.
13. Natarajan S, Priester A, Margolis D, et al. Prostate MRI and ultrasound with pathology and coordinates of tracked biopsy (prostate-MRI-US-biopsy) (version 2) [dataset]. The Cancer Imaging Archive; 2020.
14. Dice LR. Measures of the amount of ecologic association between species. *Ecology*. 1945;26:297–302.

15. Everingham M, Van Gool L, Williams CKI, et al. The Pascal visual object classes (VOC) challenge. *Int J Comput Vis*. 2010;88:303–338.
16. Bardis MD, Houshyar R, Chang PD, et al. Applications of artificial intelligence to prostate multiparametric MRI (mpMRI): current and emerging trends. *Cancers (Basel)*. 2020;12:1204. https://doi.org/10.3390/cancers12051204
17. Belue MJ, Turkbey B. Tasks for artificial intelligence in prostate MRI. *Eur Radiol Exp*. 2022;6(1):33. https://doi.org/10.1186/s41747-022-00287-9
18. Bardis M, Houshyar R, Chantaduly C, et al. Segmentation of the prostate transition zone and peripheral zone on MR images with deep learning. *Radiol Imaging Cancer*. 2021;3:e200024. https://doi.org/10.1148/rycan.2021200024
19. Yin X, Wang K, Wang L, et al. Algorithms for classification of sequences and segmentation of prostate gland: an external validation study. *Abdom Radiol (NY)*. 2024;49:1275–1287. https://doi.org/10.1007/s00261-024-04241-8
20. Belue MJ, Harmon SA, Patel K, et al. Development of a 3D CNN-based AI model for automated segmentation of the prostatic urethra. *Acad Radiol*. 2022;29:1404–1412. https://doi.org/10.1016/j.acra.2022.01.009
21. Nachbar M, Lo Russo M, Gani C, et al. Automatic AI-based contouring of prostate MRI for online adaptive radiotherapy. *Z Med Phys*. 2024;34:197–207. https://doi.org/10.1016/j.zemedi.2023.05.001
22. Xu L, Zhang G, Zhang D, et al. Development and clinical utility analysis of a prostate zonal segmentation model on T2-weighted imaging: a multicenter study. *Insights Imaging*. 2023;14:44. https://doi.org/10.1186/s13244-023-01394-w
23. Palazzo G, Mangili P, Deantoni C, et al. Real-world validation of artificial intelligence-based computed tomography auto-contouring for prostate cancer radiotherapy planning. *Phys Imaging Radiat Oncol*. 2023;28:100501. https://doi.org/10.1016/j.phro.2023.100501
24. Schelb P, Tavakoli AA, Tubtawee T, et al. Comparison of prostate MRI lesion segmentation agreement between multiple radiologists and a fully automatic deep learning system. *Rofo*. 2021;193:559–573. https://doi.org/10.1055/a-1290-8070
25. Thimansson E, Baubeta E, Engman J, Bjartell A, Zackrisson S. Deep learning performance on MRI prostate gland segmentation: evaluation of two commercially available algorithms compared with an expert radiologist. *J Med Imaging (Bellingham)*. 2024;11(1):015002. https://doi.org/10.1117/1.JMI.11.1.015002
26. Ghezzo S, Mongardi S, Bezzi C, et al. External validation of a convolutional neural network for the automatic segmentation of intraprostatic tumor lesions on ^{68}Ga-PSMA PET images. *Front Med (Lausanne)*. 2023;10:1133269. https://doi.org/10.3389/fmed.2023.1133269
27. Liu G, Pan S, Zhao R, et al. The added value of AI-based computer-aided diagnosis in classification of cancer at prostate MRI. *Eur Radiol*. 2023;33:5118–5130. https://doi.org/10.1007/s00330-023-09433-2
28. Gunashekar DD, Bielak L, Hägele L, et al. Explainable AI for CNN-based prostate tumor segmentation in multi-parametric MRI correlated to whole-mount histopathology. *Radiat Oncol*. 2022;17:65. https://doi.org/10.1186/s13014-022-02035-0
29. He K, Zhang X, Ren S, et al. Deep residual learning for image recognition. Proceedings of the IEEE Computer Society Conference on Computer Vision and Pattern Recognition. December 2016: 770-778.
30. He K, Gkioxari G, Dollar P, et al. Mask R-CNN. Proceedings of the IEEE International Conference on Computer Vision. October 2017: 2980-2988.
31. Morid MA, Borjali A, Del Fiol G. A scoping review of transfer learning research on medical image analysis using ImageNet. *Comput Biol Med*. 2020;128:104115. https://doi.org/10.1016/j.compbiomed.2020.104115
32. Singla D, Cimen F, Narasimhulu CA. Novel artificial intelligent transformer U-NET for better identification and management of prostate cancer. *Mol Cell Biochem*. 2023;478:1439–1445.
33. Andersén C, Rydén T, Thunberg P, et al. Deep learning-based digitization of prostate brachytherapy needles in ultrasound images. *Med Phys*. 2020;47:6414.
34. Li Y, Lin C, Zhang Y, et al. Automatic segmentation of prostate MRI based on 3D pyramid pooling Unet. *Med Phys*. 2023;50:906–921. https://doi.org/10.1002/mp.15895
35. Li Y, Wu Y, Huang M, Zhang Y, Bai Z. Automatic prostate and periprostatic fat segmentation based on pyramid mechanism fusion network for T2-weighted MRI. *Comput Methods Programs Biomed*. 2022;223:106918. https://doi.org/10.1016/j.cmpb.2022.106918
36. Natarajan S, Marks LS, Margolis DJ, et al. Clinical application of a 3D ultrasound-guided prostate biopsy system. *Urol Oncol*. 2011;29:334–342. https://doi.org/10.1016/j.urolonc.2011.02.014
37. Valerio M, McCartan N, Freeman A, et al. Visually directed vs. software-based targeted biopsy compared to transperineal template mapping biopsy in the detection of clinically significant prostate cancer. *Urol Oncol*. 2015;33:424. https://doi.org/10.1016/j.urolonc.2015.06.012
38. Oberlin DT, Casalino DD, Miller FH, et al. Diagnostic value of guided biopsies: fusion and cognitive-registration magnetic resonance imaging versus conventional ultrasound biopsy of the prostate. *Urology*. 2016;92:75–79. https://doi.org/10.1016/j.urology.2016.02.041
39. Puech P, Rouvière O, Renard-Penna R, et al. Prostate cancer diagnosis: multiparametric MR-targeted biopsy with cognitive and transrectal US-MR fusion guidance versus systematic biopsy–prospective multicenter study. *Radiology*. 2013;268:461–469. https://doi.org/10.1148/radiol.13121501
40. Hsieh PF, Chang TY, Lin WC, et al. A comparative study of transperineal software-assisted magnetic resonance/ultrasound fusion biopsy and transrectal cognitive fusion biopsy of the prostate. *BMC Urol*. 2022;22:72. https://doi.org/10.1186/s12894-022-01011-w
41. Yamada Y, Shiraishi T, Ueno A, et al. Magnetic resonance imaging-guided targeted prostate biopsy: comparison between computer-software-based fusion versus cognitive fusion technique in biopsy-naïve patients. *Int J Urol*. 2020;27:67–71. https://doi.org/10.1111/iju.14127
42. Checcucci E, Piramide F, Amparore D, et al. Beyond the learning curve of prostate MRI/TRUS target fusion biopsy after more than 1000 procedures. *Urology*. 2021;155:39–45. https://doi.org/10.1016/j.urology.2021.06.021